

# EPJ B

Condensed Matter  
and Complex Systems

EPJ.org

your physics journal

Eur. Phys. J. B (2020) 93: 67

DOI: [10.1140/epjb/e2020-100544-y](https://doi.org/10.1140/epjb/e2020-100544-y)

## A Hamiltonian model of the Fibonacci quasicrystal using non-local interactions: simulations and spectral analysis

Amrik Sen and Carlos Castro Perelman



# A Hamiltonian model of the Fibonacci quasicrystal using non-local interactions: simulations and spectral analysis<sup>\*,\*\*</sup>

Amrik Sen<sup>1,a</sup> and Carlos Castro Perelman<sup>2,3</sup>

<sup>1</sup> School of Mathematics, Thapar Institute of Engineering & Technology, Patiala, Punjab, India

<sup>2</sup> Centre for Theoretical and Physical Sciences, Clark Atlanta University, Atlanta, Georgia, USA

<sup>3</sup> Ronin Institute, 127 Haddon Pl., Montclair, NJ 07043, USA

Received 9 November 2019 / Received in final form 4 February 2020

Published online 8 April 2020

© EDP Sciences / Società Italiana di Fisica / Springer-Verlag GmbH Germany, part of Springer Nature, 2020

**Abstract.** This article presents a Hamiltonian architecture based on *vertex types* and *empires* for demonstrating the emergence of aperiodic order in one dimension by a suitable prescription for breaking translation symmetry. At the outset, the paper presents different algorithmic, geometrical, and algebraic methods of constructing empires of vertex configurations of a given lattice. These empires have *non-local* scope and form the building blocks of the proposed lattice model. This model is tested via Monte Carlo simulations beginning with randomly arranged  $N$  tiles. The simulations clearly establish the Fibonacci configuration, which is a one-dimensional quasicrystal of length  $N$ , as the final relaxed state of the system. The Hamiltonian is promoted to a matrix operator form by performing dyadic tensor products of pairs of interacting empire vectors followed by a summation over all permissible configurations. A spectral analysis of the Hamiltonian matrix is performed and a theoretical method is presented to find the exact solution of the attractor configuration that is given by the Fibonacci chain as predicted by the simulations. Finally, a precise theoretical explanation is provided which shows that the Fibonacci chain is the most probable ground state. The proposed Hamiltonian is a mathematical model of the one dimensional Fibonacci quasicrystal.

## 1 Introduction

The simplest geometrical method of generating a one dimensional quasicrystal, such as the Fibonacci chain, is by the cut and project procedure from a strip embedded in the two dimensional  $\mathbb{Z}_2$  lattice and with a slope proportional to the Galois conjugate  $-\frac{1}{\phi}$ , where  $\phi = \frac{1+\sqrt{5}}{2}$  is the golden mean [1,2]. The method can be replicated to generate higher dimensional quasi-lattices. However, this purely geometrical construction does not lend a physical picture of the underlying energetics of the quasicrystal configuration. Specifically, it is of immense importance to experimentalists and material scientists to understand the microscopic atomic arrangements in a quasicrystal [3,4]. Besides, a physical picture of the emergence of translation asymmetry may be of general interest to scientists striving to unravel the laws of nature through the study of symmetries and conservation principles [5–8].

### 1.1 Brief introduction to quasicrystal models

Quasicrystal models can be broadly categorized as under:

- microscopic tiling models based on matching rules [9–17],
- continuum models [8,18–20], and
- computational models based on molecular dynamics (MD) simulations of Newton's equations of motions [21,22] or Monte-Carlo (MC) methods [23,24].

Matching rules based tiling models are abstract mathematical approaches that are useful to investigate the properties of aperiodic order but by themselves they are not directly physically realizable models. Continuum models like the density wave approach involve analyzing density of the condensing liquid phase in Fourier phase space. The basic hypothesis in such approaches relies on the conservation of the free energy of the system upon a rigid translation of the cut space. A minimization of the Landau free energy in the Fourier space representation selects specific series expansion coefficients that set particular wave vectors and consequently characterize the resulting underlying stable structure which is aperiodic but ordered. The continuum models do not reveal the nature of interatomic interactions responsible for quasicrystal formation. MD simulations involve solving Newton's classical equations of motion with specifically prescribed pair potential

\* Supplementary material in the form of three mpeg files and one mp4 file available from the Journal web page at <https://doi.org/10.1140/epjb/e2020-100544-y>.

\*\* Contribution to the Topical Issue "Advances in Quasi-Periodic and Non-Commensurate Systems", edited by Tobias Stauber and Sigmund Kohler.

<sup>a</sup> e-mail: [amriksen@thapar.edu](mailto:amriksen@thapar.edu)

interactions (e.g., the Lennard-Jones-Gauss (LJG) potential [23,24]) that have local scope. The aforementioned simulations have successfully demonstrated quasicrystal growth with long range order using local interactions. The experimental plausibility of local interactions driving quasicrystal growth has also been demonstrated for the decagonal case [25]. Further, in MC simulations using the LJG potential [24], in dynamic phase field simulations in two dimensions [26], and in entropy-driven tiling models [27,28], defect free quasicrystal growth by accretion is observed. However, in atomic quasicrystals, it is believed that quantum mechanical effects may be important [29–31].

## 1.2 The Fibonacci quasicrystal

We have chosen the Fibonacci model as a subject of investigation because it is the most elementary quasicrystal model in one dimension. Even though the Fibonacci chain, defined mathematically in a subsequent section of this paper, is generally regarded as a theoretical construct to study and conceptualize aperiodic order, it has direct relevance in many physical applications as well.

The Fibonacci system is a widely studied model. Fibonacci quasicrystals have been artificially fabricated [32] and their characteristic physical and topological properties have been investigated [33,34] in the laboratory. Several authors have studied electronic structures and energy spectrum of Fibonacci quasicrystals by considering tight binding Hamiltonian models with hopping constants prescribed by a finite Fibonacci word (Fibonacci approximant) [35–39].

In this paper, we propose a tiling model in the form of an appropriate Hamiltonian for stabilizing a one dimensional random chain into the Fibonacci quasicrystal. The proposed mathematical model is based on a Hamiltonian involving non-local *empire-empire* interactions. The *empires* have a generalized geometrical notion and can be constructed for any given chain configuration of long and short tiles in one dimension (not just for the Fibonacci configuration). The proposed lattice Hamiltonian has a ground state which is the Fibonacci quasicrystal.

## 1.3 Scope of this work

The stability of quasicrystal structures is still an open problem. This research paper presents a Hamiltonian architecture using *vertex configurations* (VCs) and their respective *empires* to understand the nature of atomic re-arrangements compatible with a stable quasicrystal configuration in one dimension. The theoretical model presented here assumes non-local interactions between empire-pairs. Non-locality is manifested in the non-local scope of empires of the VCs. The proposed Hamiltonian is promoted to a matrix operator form whose constituents have a geometrical interpretation. The simulations of the proposed Hamiltonian model demonstrate the manner in which a random assortment of tiles interacts and rearranges to form a one dimensional Fibonacci quasicrystal. A detailed spectral analysis of the Hamiltonian operator reveals that the Fibonacci state is the most likely ground

state of the system. This aperiodic Fibonacci ground state can be generated entirely by the interaction of a collection of sub-states (empires) of different chain configurations undergoing energetic relaxation.

## 1.4 Organization of this paper

Section 2 introduces the definition of Fibonacci words in a recursive manner, and presents three different methods of constructing empires for a given VC in a Fibonacci chain. While the geometric method is primarily useful for implementing the Monte Carlo simulations discussed in the latter section, the algebraic expression of the empires of a Fibonacci chain will be key to understand the manner in which the translation symmetry is broken as discussed later. Section 3 discusses the implementation of the Monte Carlo simulation of the proposed Hamiltonian model and presents results of these simulations. In Section 4 the matrix operator form of the Hamiltonian and its spectral analysis is presented and these analytical results are compared with the results of the simulations. A direct physical explanation is provided as to why the Fibonacci chain is the most likely ground state of the system as is evident from the simulations. In Sections 5 and 6, a summary of the main contributions of this paper is presented and future plans to extend the work to two dimensional quasicrystals are outlined.

At the very outset, it must be carefully noted that unless otherwise specified, by the phrase *Fibonacci chain*, we refer to the finite Fibonacci approximant in this article. This terminology is interchangeably used with equivalent phrases such as *Fibonacci configuration* and *Fibonacci state*.

## 2 The Fibonacci lattice

A Fibonacci sequence is constructed from the Fibonacci numbers by using the following recurrence relation,

$$F_{n+1} = F_n + F_{n-1}, \quad (1)$$

where  $F_0 = 0, F_1 = 1$ . An interesting property of this sequence is the golden ratio scaling,  $\lim_{n \rightarrow \infty} \frac{F_{n+1}}{F_n} = \phi$  where the rapid convergence to  $\phi$  (the golden ratio) can be verified in a simple manner. A Fibonacci word is constructed using the following recurrence relation,

$$S_n = S_{n-1}S_{n-2}, \quad n \geq 2, \quad (2)$$

with  $S_0 = 0, S_1 = 01$ . Thus, a Fibonacci word of length  $n$  is a finite sequence of 0 and 1 constructed as above [40,41]. The relationship between a finite Fibonacci word and the Fibonacci sequence stems from the fact that the length of  $S_n$  is  $F_{n+2}$ , the  $(n+2)$ th Fibonacci number. A Fibonacci lattice or Fibonacci quasicrystal of size  $n$  is a lattice with grid spacing encoded by the Fibonacci word  $S_n$  where  $0 \rightarrow \phi$  and  $1 \rightarrow 1$ . A standard representation of such a quasi lattice is given by replacing 0 by  $L$  and 1 by  $S$  where the symbols  $L$  and  $S$  are regarded as *tiles*. E.g., a section of a Fibonacci quasicrystal in the  $L, S$  representation looks

$V$ :	set of VCs (vertex configurations) = $\{\{L, L\}, \{L, S\}, \{S, L\}\}$
$X$ :	set of coordinates denoted by subscript numerals, i.e. $(x_0, x_1, x_2, \dots) \equiv (0, 1, 2, \dots)$
$\alpha_j$ :	the VC $\alpha$ located at coordinate $j$
$E_{\alpha_j, l}$ :	$\begin{cases} +1, & \text{if tile located at } l \text{ is } S \\ -1, & \text{if tile located at } l \text{ is } L \\ 0, & \text{otherwise (i.e. unforced tile)} \end{cases}$
$\tau_i$ :	binary representation of the tiling space with entries 1 for $S$ and $-1$ for $L$
$\Omega$ :	domain of the lattice containing the set $\{\alpha_i\}_{i=2:N}$ where $N$ is the length of the lattice

like ...LSLLSLSLLSLLS... . Thus, a Fibonacci lattice is a quintessential example of a one dimensional quasicrystal.

## 2.1 Vertex configurations and empires

The model demonstrated in this manuscript is designed based on VCs and empires. These are standard canonical descriptors of quasicrystals [42]. For the 1D Fibonacci quasicrystal, there are three VCs, viz.,  $\{L, L\}$ ,  $\{L, S\}$ ,  $\{S, L\}$ . Note that the tile  $S$  cannot appear in succession in a Fibonacci lattice and hence  $\{S, S\}$  is not a legal VC.

### 2.1.1 Notations and definitions

#### 2.1.1.1 Empire

Corresponding to each vertex type (vertex configuration) at each coordinate, there is a set of *forced* tiles that constitute the respective empire [43–48]. The precise formulation of an empire for a given VC will become clear through the detailed discussions of this section.

Generally speaking, there are three ways of constructing empires of a VC in a quasicrystal. For the one dimensional case, a simple substitution rule may be used to enlist the empires for any vertex configuration [2]. Alternatively, a geometric method using an irrational projection from a two dimensional lattice may be used to generate the empires of a given VC [49,50]. Finally, a set of algebraic formulae for the empires of the one dimensional Fibonacci quasicrystal is developed and presented here. All these methods are discussed in an elaborate manner in the context of the one dimensional Fibonacci quasicrystal.

In what follows, the mathematical notation and definitions of the related terms are given below.

See equation (3) above.

For the sake of notational brevity, a tile referenced by the coordinate  $l$  means that the tile is located between the lattice coordinates  $l$  and  $l+1$  for a right sided entry and between the coordinates  $-l$  and  $-l-1$  for a left sided entry. For example, consider the chain expressed by (5). The tile referenced by  $l=1$  is  $S$  located between  $l=1$  and  $l+1=2$ .<sup>1</sup> A VC referenced by coordinate  $j$  refers to the one composed of the tiles on either side of  $j$ . Finally,

<sup>1</sup> Left and right sided entries in an empire vector are with reference to the coordinate located at the center of the VC, this is analogous to a *radial* convention with the center of the VC as the origin.

the VC-empire parameterization encompasses the local and non-local *field of influence* of a given VC through its domain of influence by the forced tiles. Concisely, this empire *field* of VC  $\alpha$  situated at  $j$  is denoted by the empire vector

$$\mathbf{E}_{\alpha_j} = (\dots E_{j,-2}^{\alpha L} E_{j,-1}^{\alpha L} E_{j,0}^{\alpha L} E_{j,1}^{\alpha R} E_{j,2}^{\alpha R} \dots),$$

where superscripts  $L$  and  $R$  refer to left and right sided entries respectively. In the following three sections, we discuss three different methods of finding the empires of VCs. The substitution method and the geometric method of constructing empires have been explored by others in the past but the algebraic prescriptions of the empires are new results presented here.

### 2.1.2 Substitution algorithm for constructing empires

This algorithm borrows extensively from detailed discussions on substitution rules for generating aperiodic Fibonacci words in chapter 4 of the text by Baake and Grimm [2]. This method is applicable for the one dimensional Fibonacci chain but may be extended as a principle to a network of Fibonacci chains. The identification of the empire tiles in a real Fibonacci chain, denoted by uppercase  $S$  and  $L$  tiles, is undertaken by referencing from a virtual Fibonacci chain, denoted by lowercase  $s$  and  $l$  tiles. The virtual chain (hitherto referred to as **fibonacci**) begins with the tile  $l$  and is constructed by using the substitution rule  $l \rightarrow ls$ ,  $s \rightarrow l$  iteratively. Thus the first few iterations give  $lsllslls$  because  $l \rightarrow ls \rightarrow lsl \rightarrow lslls \rightarrow lsllslls$ . The VCs along with their respective empires can be expressed algorithmically as follows.

$$\begin{aligned} \{L, L\}s + \text{fibonacci} &\rightsquigarrow \begin{cases} s \rightarrow SL \\ l \rightarrow (LS|SL)L \end{cases} \\ \{L, S\}L + s + \text{fibonacci} &\rightsquigarrow \begin{cases} s \rightarrow (LS|SL)L \\ l \rightarrow (LSLS|SLSL|SLLS)L \end{cases} \\ \{S, L\}s + \text{fibonacci} &\rightsquigarrow \begin{cases} s \rightarrow (LS|SL)L \\ l \rightarrow (LSLS|SLSL|SLLS)L \end{cases} \end{aligned} \quad (4)$$

Here, each line of the algorithm must be read as follows. E.g., the first line means: “the empire of a given  $\{L, L\}$  VC in a real Fibonacci chain is constructed by the substitution  $\{L, L\} \rightarrow LL$ , and  $s \rightarrow SL, l \rightarrow (LS|SL)L$  performed on the virtual fibonacci chain  $s + \text{fibonacci}$  where the

$$\dots L_1 \underbrace{L_2}_{\substack{\mathbf{L}_1 \\ E_{0,0}^{1L}}} \underbrace{L_3}_{\substack{\mathbf{L}_2 \\ E_{0,0}^{1R}}} S L_4 \dots L_5 \dots L_6 \dots L_7 \dots L_8 \dots . \quad (6)$$

$$\begin{aligned} \mathbf{E}_0^1 = \{E_{0,l}^1\}_{l \in X, X \in \Omega} &= (\dots E_{0,-5}^{1L} E_{0,-4}^{1L} E_{0,-3}^{1L} E_{0,-2}^{1L} E_{0,-1}^1 E_{0,0}^{1L} E_{0,0}^{1R} E_{0,1}^{1R} E_{0,2}^{1R} E_{0,3}^{1R} E_{0,4}^{1R} E_{0,5}^{1R} \dots) \\ &= (\dots 0 \ 0 \ -1 \ 1 \ -1 \ 0 \ 0 \ -1 \ 1 \underbrace{-1}_{E_{0,0}^{1L}} \underbrace{-1}_{E_{0,0}^{1R}} \ 1 \ -1 \ 0 \ 0 \ -1 \ 1 \ -1 \ 0 \ 0 \dots) \end{aligned} \quad (7)$$

forced tiles are expressed without parenthesis, the operation  $|$  means *conditional OR*, and  $\rightsquigarrow$  stands for the above mentioned substitution.” Above, only a right sided empire identification procedure has been shown but extension to the left of the VC is straightforward by symmetry consideration. This is made clear in the example presented in the following section.

### *2.1.2.1 Illustration of the algorithm*

Consider a given section of a 1D Fibonacci chain (labelled as the real chain):

See equation (5) above.

where the bold font tiles  $\mathbf{L}_0 \mathbf{L}$  constitute the VC of interest located at the coordinate  $x_0 \equiv 0$  in this example. The underset numerals denote coordinate locations (recall that the tiles are indexed by the coordinates to their immediate left). The significance of the underset uparrows  $\uparrow$  is explained after expression (7). The 1D Fibonacci chain in (5) is represented in tiling space. The equivalent binary representation of the chain is a sequence  $\{\tau_i\}$  with entries  $\pm 1$  depending on the corresponding entries in the tiling space, i.e.,  $-1$  for  $L$  and  $1$  for  $S$ . Thus, we have  $\tau_{-3} = 1, \tau_{-2} = -1, \tau_{-1} = 1, \tau_0 = -1, \tau_1 = -1, \tau_2 = 1, \tau_3 = -1, \dots$  etc.

The first step involves the construction of the virtual Fibonacci chain that serves as a guide to identify the forced tiles in the real chain and thereby the corresponding empire. The algorithm prescribes the form of the virtual chain to be  $s + \text{fibonacci}$  where **fibonacci** begins with the tile  $l$  and is constructed by using the substitution  $l \rightarrow ls$ ,  $s \rightarrow l$  iteratively as mentioned earlier. Thus we have the following virtual chain,

$$s + lsllsllsll\ldots = slsllsllsll\ldots .$$

The substitution rule for  $\{L, L\}$  is applied to the above virtual chain, i.e.  $s \rightarrow SL, l \rightarrow ()()L$  where each  $()$  corresponds to one unforced tile. Further, the unforced tiles are labelled by 0s for convenience. This entails the following empire form.

*See equations (6) and (7) above.*

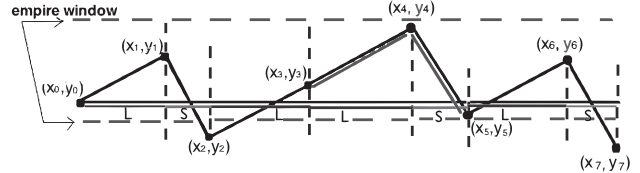


**Fig. 1.** (Not to scale) Proof of concept of the cut and project method to find the empire of a given vertex configuration,  $\{L, S\}$ , bounded by the lattice coordinates  $(x_3, y_3), (x_4, y_4)$  and  $(x_5, y_5)$ . The empire window depicted by the horizontal dashed lines is bounded by the maximum and minimum  $y$ -coordinates of the lattice points defining the VC, shown here by solid double lines (oblique) bounded by the horizontal dashed lines. Tiles that have both their bounding coordinates within this empire window constitute the empire of the given VC. Thus, for the string shown here, the section of the empire corresponding to the  $\{L, S\}$  VC is: ... $L()$ ...**LSL()**....

The tiles bearing the underset uparrows  $\uparrow$  are the forced tiles of the VC **LL**. The corresponding tiles in the real chain (5) are consequently indexed by the uparrows  $\uparrow$  and constitute the forced tiles of the empire of the VC **LL**. The coordinate locations for the chain in (6) are implied as in (5) and are not shown again. In terms of the vectorial notation, the empire for  $\{L, L\}$  located at  $j = 0$  is given by equation (7).

### 2.1.3 Geometric method of constructing empires

The cut and project method of constructing the empire of a given vertex configuration is illustrated in this section. This method can be applied for any chain (not necessarily a Fibonacci chain). It may be recalled that a 1D Fibonacci chain can be constructed by projecting a two-dimensional cylindrical section of the  $\mathbb{Z}_2$  lattice onto a 1D real line by using an irrational angle [1,2]. Hence, it is reasonable to search for the forced tiles that constitute the empire of a given vertex type within this band of the original  $\mathbb{Z}_2$  lattice. For convenience of calculation, we consider a rotated frame of reference of the original  $\mathbb{Z}_2$  lattice (a.k.a. mother lattice) such that the horizontal  $x$ -axis of the new 2D plane coincides with the projected quasicrystal space of the Fibonacci chain (refer Fig. 1). In this frame, the horizontal and vertical arms of the  $\mathbb{Z}_2$  lattice appear at an irrational angle with respect to

the  $x$ -axis as is further illustrated in the graphic depicted in Figure 1. The lattice arm joining points  $(x_0, y_0)$  and  $(x_1, y_1)$  makes an angle  $\theta = \tan^{-1} \frac{1}{\phi}$  with the horizontal axis. Here  $\phi = \frac{1+\sqrt{5}}{2}$ . Moreover, the lattice arms are each of unit length and orthogonal to each other. The arm joining the points  $(x_2, y_2)$  and  $(x_1, y_1)$  also makes the same angle  $\theta$  with the vertical.

Given the state of a two-alphabet chain (Fibonacci or otherwise) in 1D, the first step involves reconstructing the corresponding section of the  $\mathbb{Z}_2$  lattice, i.e., the  $(x, y)$  coordinates in the original 2D space. Following Figure 1 and simple trigonometry, we obtain the following relations,

$$\begin{aligned} y_i &= y_{i-1} - \tau_i \sin(\Theta_i \pi/2 + \theta), \quad \Theta_i = \frac{1 + \tau_i}{2}, \\ x_i &= x_{i-1} - \kappa_i \tau_i, \quad \kappa_i = \begin{cases} 1, & \text{if } \tau_i = -1 \\ -\frac{1}{\phi}, & \text{if } \tau_i = 1. \end{cases} \end{aligned} \quad (8)$$

The starting point of the chain is located at the origin, i.e.,  $(x_0, y_0) = (0, 0)$ .

Next, the calculation of the empire is undertaken by identifying the bounding  $(x, y)$  coordinates of the VC in question for which we intend to find the empire. The empire window is constructed in the 2D plane by finding the minimum and the maximum of the  $y$ -coordinates associated with the VC. This is illustrated graphically in Figure 1. The tiles with both bounding  $(x, y)$  coordinates within the empire window constitute the empire of the given VC. It is important to emphasize that this method of finding the empires is not restricted to a Fibonacci chain alone but is more general and works for any 2-alphabet chain.

#### 2.1.4 Algebraic formulae of empires

This section presents analytic expressions of the empires for the Fibonacci quasicrystal and thereby prescribes the exact form by which the translation symmetry is absent. It must not be surprising that the expressions are related to the Fibonacci word. The empires obtained by using these formulae are validated against the corresponding empires constructed by two other methods explained above. In the following paragraphs, we illustrate the algebraic forms of the empires for each VC of the chain.

##### 2.1.4.1 Symmetric VC, $\{L, L\}$

We provide a direct analytical expression for every element of the empire vector  $\mathbf{E}_j^\alpha$ . For example, the  $(l - j - 1)$ th entry of the empire vector  $\mathbf{E}_j^{1R}$  (for VC  $\{L, L\}$ ) is given by

$$\begin{aligned} E_{j,l}^{1R} &\equiv E_n^{1R} = f_{n+1}(f_n + f_{n-1}) - f_n, \\ n &= l - j > 0, \\ E_{0,0}^{1R} &= E_0^{1R} = -1 \text{ (by construction)}, \end{aligned} \quad (9)$$

where  $f_n$  is the  $n$ th bit of an infinite Fibonacci word<sup>2</sup>

$$f_n = 2 + u_n - u_{n+1}, \quad u_n = \lfloor n\phi \rfloor,$$

$\phi$  is the golden ratio  $\frac{1+\sqrt{5}}{2}$ . The superscript  $R$  denotes empire entries to the *right* of the VC located at  $j$  including the right tile of the concerned VC. Also note that  $f_0 = 1$ , i.e. the 0th bit of a Fibonacci word is taken as 1 by prepending 1 to the Fibonacci word defined by the recursion (2),  $f_1 = 0$ ,  $f_2 = 1$ , etc..  $\lfloor \cdot \rfloor$  is the standard *floor* operator that outputs the integer part of the argument. For consistency, entries from equation (9) are compared with that of entries from equation (7).  $E_{0,0}^{1R} = -1$ ,  $E_{0,1}^{1R} = 1(0+1) - 0 = 1$ ,  $E_{0,2}^{1R} = 0(1+0) - 1 = -1$ ,  $E_{0,3}^{1R} = 0(0+1) - 0 = 0$ ,  $E_{0,4}^{1R} = 1(0+0) - 0 = 0$ ,  $E_{0,5}^{1R} = 0(1+0) - 1 = -1$ .

Owing to the symmetry of the  $\{L, L\}$  VC, using  $f_{-n} = f_n$  in conjunction with the formula given by equation (9), gives the entries of the empire vector to the left of  $\mathbf{LL}$ . For a symmetric VC like  $\{L, L\}$ , the following is trivially true:  $E_{-n}^{1L} = E_n^{1R}$ . Here  $L$  corresponds to left and the convention for referencing the tiles is the following:

- tiles to the right of the VC are referenced by the coordinate  $x_l$  to their immediate left, and
- tiles to the left of the VC are referenced by the coordinate  $x_l$  to their immediate right,

i.e. the convention follows a radial indexing scheme with the center of the VC located at  $x_j$  ( $x_0$  in the above example) as the origin. Additionally,  $E_{0,0}^{1R} = E_{0,0}^{1L}$ , each referencing the right and left tiles that respectively constitute the VC. Finally,  $\mathbf{E}_j^1 = \mathbf{E}_j^{1L} + \mathbf{E}_j^{1R}$  constitutes the full empire vector. Here

$$\mathbf{E}_{j=0}^{1L} = (\dots E_{0,-5}^{1L} E_{0,-4}^{1L} E_{0,-3}^{1L} E_{0,-2}^{1L} E_{0,-1}^{1L} E_{0,0}^{1L} 0 0 0 0 0 0 \dots)$$

and likewise for  $\mathbf{E}_{j=0}^{1R}$ . For brevity, the superscripts  $L$  and  $R$  are often omitted and the sign of the subscript  $n = l - j$  is sufficient to identify the left and right tiles.

##### 2.1.4.2 Asymmetric VC, $\{L, S\}, \{S, L\}$

Similarly, exact formulations of the asymmetric VCs are given below.

$$\begin{aligned} E_n^{3R} &= \begin{cases} -1; & n = 0 \\ 3 + u_n - u_{n+2}; & n \geq 1, \end{cases} \\ E_n^{2R} &= \begin{cases} 1; & n = 0 \\ -1; & n = 1 \\ E_{n-1}^{3R}; & n > 1. \end{cases} \end{aligned} \quad (10)$$

By symmetry, the left sided entries are

$$\begin{aligned} E_{-n}^{3L} &= E_n^{2R}, \quad n \geq 0 \\ E_{-n}^{2L} &= E_n^{3R}, \quad n \geq 0. \end{aligned} \quad (11)$$

<sup>2</sup>The first few entries of an infinite Fibonacci word are 1, 0, 1, 0, 0, 1, 0, 1, 0, 0, 1, 0, 1, 0, 1... after prepending by 1 that is now taken as the 0th bit of an infinite Fibonacci word.

Clearly, the non-trivial empire tiles obey the following relations  $E_{-n}^3 = E_n^2$ ,  $E_{-n}^2 = E_n^3$ ,  $n > 0$ . Moreover,  $\mathbf{E}_j^\alpha = \mathbf{E}_j^{\alpha L} + \mathbf{E}_j^{\alpha R}$  constitutes the full empire vector for the VCs  $\alpha = 2, 3$ . The definitions of  $u_n$ ,  $\mathbf{E}_j^{\alpha L}$  and  $\mathbf{E}_j^{\alpha R}$  are as described earlier. Note that for an asymmetric VC, the 0th mode empire tiles  $\mathbf{E}_{0,0}^{\alpha L} \neq \mathbf{E}_{0,0}^{\alpha R}$  are defined as above. This completes the parametrization of the 1D Fibonacci chain in terms of the VCs and the corresponding empires.

## 2.2 Random flips

The Monte Carlo simulations of Section 3 below employ random flips to span the different chain configurations. A random flip can be categorized as follows:

- **symmetric flip:** For the 1D case, this refers to the flips of the type  $\{L, S\} \leftrightarrow \{S, L\}$ . A flip of this kind preserves the local length at the location of the flip.
- **asymmetric flip:** This refers to the flips of the type  $\{L, L\} \leftrightarrow \{S, L\}$  or  $\{S, L\} \leftrightarrow \{L, L\}$ , etc. A flip of this kind does not preserve the length of the quasicrystal section locally.

## 3 Hamiltonian

The canonical Hamiltonian  $H_\Omega$  for the 1D Fibonacci system is constructed as follows:

$$\begin{aligned} H_\Omega = & -\frac{1}{N} \underbrace{\sum_{k,i \in X} B_{k,i} E_{\alpha_k, i}}_{\text{interaction free terms}} - \frac{1}{N} \underbrace{\sum_{j,i \in X} J_{j,i} \langle \mathbf{E}_{\alpha_j} | \mathbf{E}_{\alpha_i} \rangle}_{\text{interaction terms}} \\ \equiv & -\frac{1}{N} \underbrace{B_{k,i} E_{\alpha_k, i}}_{\text{Einstein summation notation}} - \frac{1}{N} J_{j,i} \langle \mathbf{E}_{\alpha_j} | \mathbf{E}_{\alpha_i} \rangle, \end{aligned} \quad (12)$$

where  $B_{k,i}$  and  $J_{j,i}$  are the free parameters of the model with units of energy and  $\mathbf{E}_{\alpha_j} \equiv \mathbf{E}_j^\alpha$  is a dimensionless vector of 0s and  $\pm 1$ s denoting the empire of the VC  $\alpha$  located at  $j$ . Here,  $\langle \cdot | \cdot \rangle$  denotes an inner product operation:  $\langle \mathbf{A} | \mathbf{B} \rangle := \sum_i A_i B_i$ , where  $\mathbf{A}, \mathbf{B}$  are vectors with entries  $A_i$  and  $B_i$  respectively. The locations of the forced tiles are referenced by the elements  $\pm 1$  in the vector  $\mathbf{E}_{\alpha_j}$  depending on whether the forced tile in question is  $S$  or  $L$ . The Hamiltonian in equation (12) has two terms, viz., the interaction free term which expresses the energy of a given VC (in conjunction with its empire field) in an external field or in vacuum, and the interaction term that encompasses the mutual energy of interaction of two distinct VCs through the interaction of their respective empires. It is important to note that by construction, the empire interactions are non-local because the values of  $m$  and  $n$  can be far apart.

### 3.1 Metropolis-Hastings simulation of the Hamiltonian

The algorithm first chooses selection probabilities  $p_s(\mu, \nu)$  which represent the probability that state  $\nu$  is selected by

the algorithm out of all states given that the previous state is  $\mu$ . It then uses acceptance probabilities  $p_a(\mu, \nu)$  that ensure the detailed balance condition.

#### 3.1.1 Simulation steps

- A lattice site is randomly picked from the Fibonacci grid using selection probability  $p_s(\mu, \nu)$  and the contribution to the total energy involving the VC at this site is calculated.
- The VC is flipped and the new contribution to the energy is calculated. The flip may be  $LL \rightarrow LS, LS \rightarrow SL, SL \rightarrow LL$ , etc.
- If the new energy is less, then the flipped value is retained.
- If the new energy is more, then the flipped value is retained with probability  $e^{-\beta(H_\nu - H_\mu)}$ . Here  $\beta = \frac{1}{k_B T}$  where  $k_B$  is the Boltzmann's constant and  $T$  is the temperature.
- The process is repeated until a global minimum of the total energy is attained.

## 3.2 Simulation parameters

Parameter	Value
$B_{k,i} \equiv B$	0 or 1
$J_{j,i} \equiv J$	1
T	0.6
N	$21^\dagger$

<sup>†</sup>  $N = 21$  corresponds to the simulation shown in Figures 2 and 3. The source files used for developing and running the simulations are freely available in a GitHub repository.<sup>3</sup>

The choice of unit coupling constants  $J_{j,i}$  is natural and ensures equal weight to the interactions between empires of pairs of VCs irrespective of their location in the chain.

## 3.3 Results of simulations

Several simulation runs with chains of different lengths ( $N = 5, 8, 13, 21, 34, 55, 89, 144$ , and 233) were performed starting with different initial states of the chain. In each case, the attractor, that minimized the total Hamiltonian, was found to be the Fibonacci chain. In Figures 2 and 3, an example of one such simulation with  $N = 21$  is presented. A selected number of movies of the simulations can be found in the first author's youtube channel.<sup>4</sup>

## 3.4 Distribution of the attractor and invariance of the Hamiltonian to initial conditions

It is important to note that by establishing the Fibonacci chain (a.k.a. the Fibonacci state) as the attractor of the Hamiltonian (12), as shown by the simulations, we are essentially interested in the relative distribution of the  $L$  and  $S$  tiles. In the next section, we invoke the ansatz that

<sup>3</sup> [https://github.com/amriksen/Fibonacci\\_Ham\\_code\\_web](https://github.com/amriksen/Fibonacci_Ham_code_web)

<sup>4</sup> <https://www.youtube.com/watch?v=MirQPchbo7Q>

<https://www.youtube.com/watch?v=1n-je95jOlk>

[https://www.youtube.com/watch?v=\\_KsToOQs5hc](https://www.youtube.com/watch?v=_KsToOQs5hc)

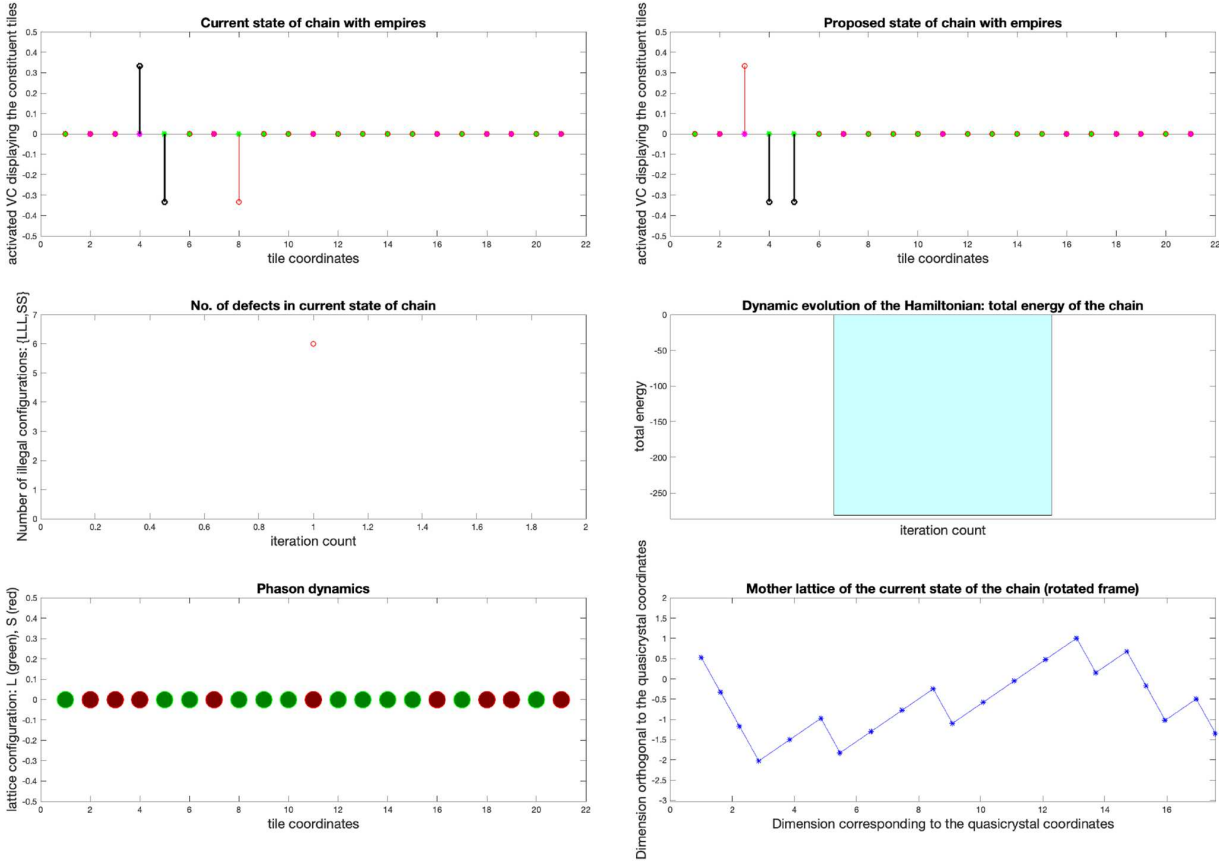


**Fig. 2.** The set of plots corresponds to the *initial state* of a chain of length  $N = 21$  (bottom left panel) at the start of the simulation where the tiles  $L$  and  $S$  are color coded as green and red respectively. The VC pairs being flipped are shown by the black colored stem pairs displayed in the top panels. The number of defects in the current state of the chain corresponds to the number of forbidden elementary configurations ( $LLL$  and  $SSS$ ) in a Fibonacci chain. The coordinates of the 2D lattice (mother lattice, ref. Fig. 1), from which the current state of the chain may be constructed, are shown in the bottom right panel. The total Hamiltonian of the current configuration is displayed in the middle right panel.

the distribution of the sign of the entries of the most relevant eigenvector of the Hamiltonian matrix prescribes the attractor configuration. The applicability of this ansatz is found to be consistent by treating the Hamiltonian as a quantum mechanical system and verifying one of the main axioms of probability as discussed in the subsequent section. It must be noted that the choice of labels for the ternary system used in the definition of the empires in Section 2.1 is entirely arbitrary and a matter of computational convenience. It must be emphasized that the results of the simulations are invariant to the initial state of the chain as is shown by the above cited movies of the simulations and Figures 2 and 3.

#### 4 Empire dyads, spectral analysis, and the Fibonacci state

In order to formulate an algebraic representation of the Fibonacci system and the associated empire dyads, it is essential to promote the Hamiltonian defined by equation (12) to a matrix operator form. Moreover, since

the external field  $B_{\alpha_k, i}$ , plays no influence on the final attractor configuration, the interaction free term will be omitted from consideration in the theoretical analysis of the Hamiltonian presented in this section. This is a matter of convenience without any loss of generality. Thus, in the absence of the external field  $B \equiv 0$ , we will present an interpretation akin to quantum mechanics in the spirit of the discussions in the literature [51–53].

##### 4.1 Construction of empire dyads and the Hamiltonian matrix operator

Consider any chain (not necessarily Fibonacci) of fixed length  $N$  (i.e.  $N$  lattice sites) where  $N$  is moderately large. The matrix operator, corresponding to a pair of interacting empire vectors<sup>5</sup> of VCs  $\alpha$  and  $\beta$  located at positions

<sup>5</sup> Note that the geometric method of constructing empires enables us to find the empire of a VC located at a certain coordinate of any chain configuration. Hence, the notion of empires is not restricted to a Fibonacci quasicrystal but applies to any configuration of the chain.

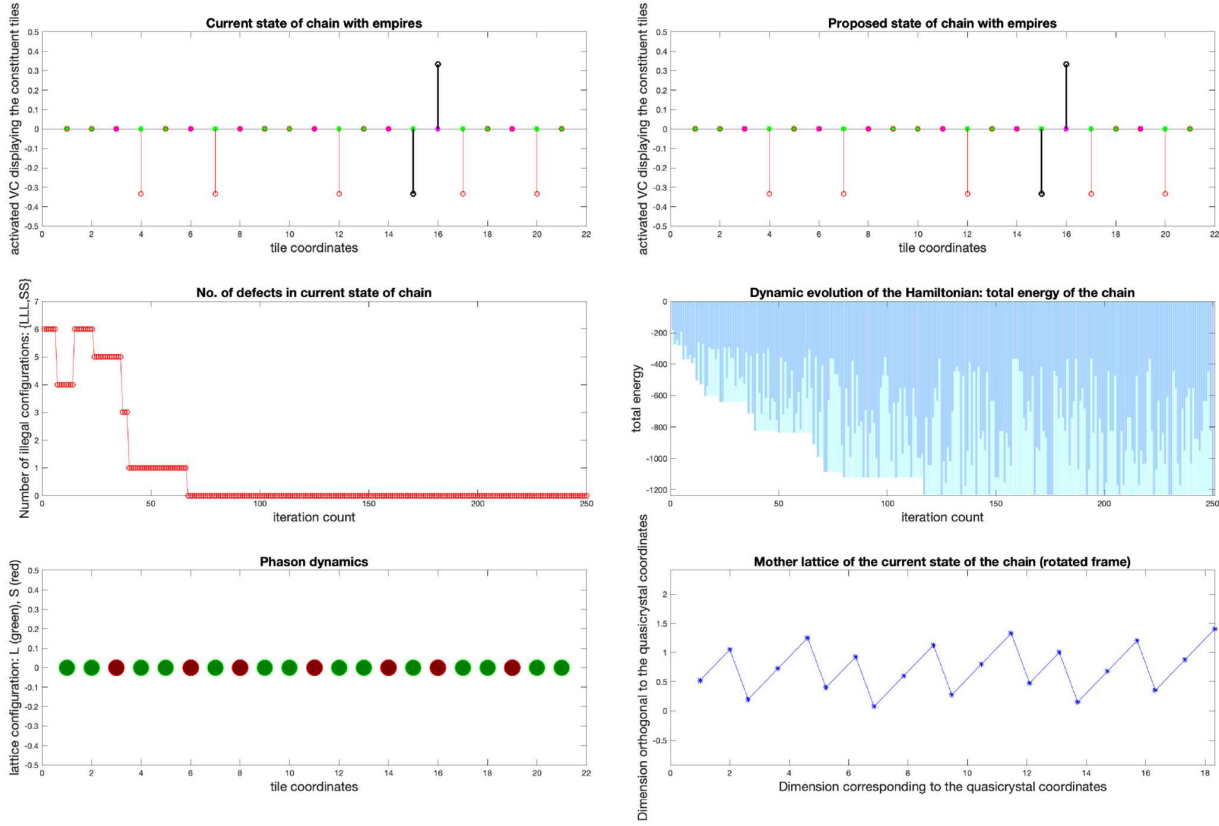


**Fig. 3.** The set of plots here corresponds to the *final relaxed state* of the chain shown in Figure 2. The arrangement of the green ( $L$ ) and red ( $S$ ) balls clearly shows that the attractor configuration is the Fibonacci chain. The evolution of the total Hamiltonian of the system is also displayed clearly demonstrating that the attractor configuration has the minimum energy. The defect counter shows the absence of any forbidden configuration in the final state and hence is consistent with the fact that the attractor is the Fibonacci chain.

$m$  and  $n$  respectively, is a *dyad* and is defined as

$$\mathcal{E}_{\alpha_m \beta_n} := \mathbf{E}_{\alpha_m} \otimes \mathbf{E}_{\beta_n} \equiv \mathbf{E}_{\alpha_m} \mathbf{E}_{\beta_n}^T. \quad (13)$$

Unlike in the earlier sections, here the coordinate locations of the individual tiles are referenced from the left (beginning of the chain), e.g. the subscript above identifies the location of the  $\alpha$  VC as the  $m$ th coordinate and so on. The empire matrix  $\mathcal{E}_{\alpha_m \beta_n}$  is a *dyadic product* of two vectors resulting in a tensor of rank two and dimensions  $N \times N$ .

The Hamiltonian operator can be then written as the distributed sum of the symmetrized Empire matrices  $\mathcal{E}_{\alpha_m \beta_n}$  over all possible VCs and location pairs as follows:

$$\mathcal{H} := -\frac{1}{N} \sum_{m,n \in X} \frac{\mathcal{E}_{\alpha_m \beta_n} + (\mathcal{E}_{\alpha_m \beta_n})^T}{2}, \quad (14)$$

where the sum is over all possible pairs of interacting empires of the given chain.  $\mathcal{H}$  is an  $N \times N$  symmetric matrix whose trace gives the Hamiltonian  $H_\Omega$  defined

by equation (12), i.e.  $H_\Omega := \text{Tr}(\mathcal{H})$ . Since the interaction free term of the Hamiltonian prescribed earlier by equation (12) plays no discernible influence on the evolution of the tiled chain into the Fibonacci configuration, it is omitted from consideration here and only the bilinear interaction terms are retained. Further, the interaction coefficients  $J_{m,n}$  that appear in the equation (12) are set to unity. Among all possible chain configurations, the Fibonacci chain corresponds to the configuration that minimizes the trace  $H_\Omega = \text{Tr}(\mathcal{H})$  as demonstrated by the Monte Carlo simulations of Section 3.3.

#### 4.2 Spectrum of the Hamiltonian $\mathcal{H}$ and theoretical analysis

In this section we will establish a few key points:

- the matrix operator form of the Hamiltonian  $\mathcal{H}$  will enable us to *theoretically* validate the results of the simulations presented in the previous section,
- the construction of  $\mathcal{H}$  given by expression (14) is correct and consistent with the construction of the Hamiltonian  $H_\Omega$  given by expression (12),

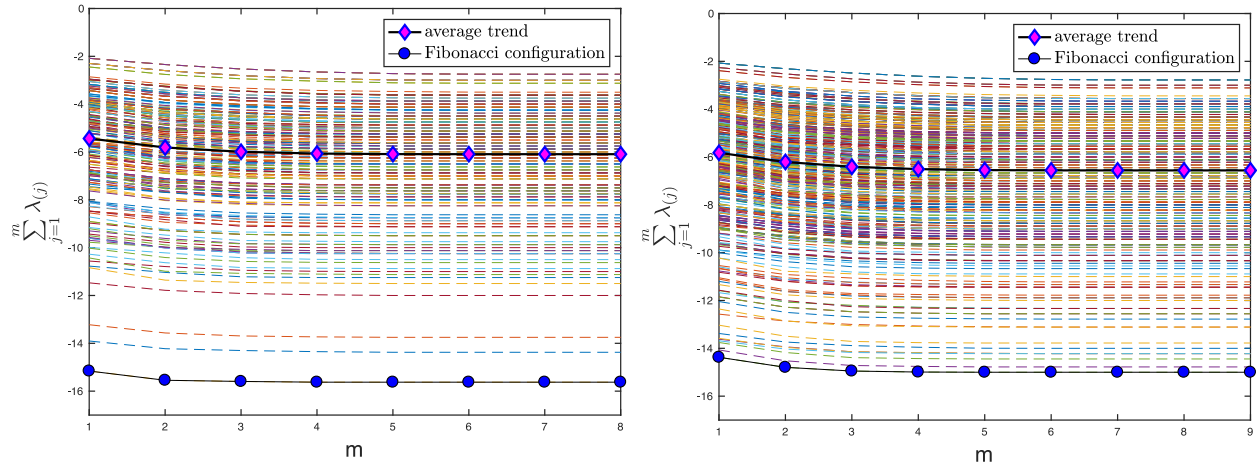


**Fig. 4.** Cumulative eigenspectrum of  $\mathcal{H}$  for different chain configurations clearly shows that the total energy given by  $H_\Omega = \text{Tr}(\mathcal{H})$  is minimized by the Fibonacci configuration. Length of the chain  $N = 8$  (left) and  $N = 9$  (right). In each case, all  $2^N$  different configurations are considered.

- the matrix  $\mathcal{H}$  encodes the energetics of different chain configurations succinctly in the form of empires, and
- spectral analysis of  $\mathcal{H}$  gives us the analytic solution of the stable chain configuration which turns out to be the Fibonacci configuration.

Further, it must be emphasized that since the geometric method allows us to construct empires of a given VC for *any* chain configuration of long and short tiles, the construction of  $\mathcal{H}$  is generally applicable to any chain configuration. Consequently, the analysis here demonstrates that the Fibonacci state emerges naturally from the model Hamiltonian as the stable solution.

#### 4.2.1 Eigenspectrum of $\mathcal{H}$ for all chain configurations

The Hamiltonian  $\mathcal{H}$  can be diagonalized as  $\Psi D \Psi^{-1}$  where the energy eigenvalues are given by the diagonal matrix

$$D = \begin{pmatrix} \lambda_{(1)} & 0 & \cdots & 0 \\ 0 & \lambda_{(2)} & \cdots & 0 \\ .. & .. & \cdots & .. \\ 0 & .. & \cdots & \lambda_{(N)} \end{pmatrix} \equiv \begin{pmatrix} E_1 & 0 & \cdots & 0 \\ 0 & E_2 & \cdots & 0 \\ .. & .. & \cdots & .. \\ 0 & .. & \cdots & E_N \end{pmatrix},$$

and  $\Psi$  is a matrix whose columns are the eigenvectors  $\psi_n$  corresponding to the eigenvalues  $\lambda_{(n)} \equiv E_n$ . By convention, we have  $|\lambda_{(1)}| \equiv |E_1| \geq |\lambda_{(2)}| \equiv |E_2| \geq |\lambda_{(3)}| \equiv |E_3| \geq \dots$ . Since  $\mathcal{H}$  is a real symmetric matrix, it has real eigenvalues with  $\lambda_{(1)} = \lambda_{\min} < 0$  corresponding to the ground state energy level  $E_1 \equiv E_{\min}$ .

To illustrate the distinct energy levels of different configurations of a chain of fixed length  $N$ , we calculate the matrix Hamiltonian  $\mathcal{H}$  as prescribed by the expression (14) for every chain configuration. This is followed by computing the eigenspectrum of  $\mathcal{H}$  for each of  $2^N$  possible configurations. The cumulative eigenspectrum corresponding to each such configuration is plotted in

Figure 4 for  $N = 8$  and  $N = 9$ . This theoretical analysis is consistent with the results of the simulation presented in the previous section. In what follows here, we show that the ground state prescribes the stable Fibonacci configuration.

#### 4.2.2 Eigenstates of $\mathcal{H}$ prescribe stable chain configuration

The results and analysis of Sections 3 and 4.2.1 demonstrate that the stable chain configuration corresponds to the state that minimizes  $H_\Omega = \text{Tr}(\mathcal{H})$ . Having obtained this energetically favored configuration, we next demonstrate how the eigenstates corresponding to this optimal configuration prescribe the Fibonacci solution state. Of course, we could simply read off the configuration with the least energy and show that it is the Fibonacci state. However, we wish to clarify two subtle points in the following analysis:

- the collection of empires corresponding to the minimum energy state would be sufficient to recover the full stable solution because  $\mathcal{H}$  is built entirely and solely from empires, and
- the Fibonacci configuration not only minimizes the total energy as shown above but also minimizes the ground state among all possible configurations.

The analysis presented below reveals that the chain has the highest probability of being in the ground state. This fact along with the second point above imply that the Fibonacci configuration is the most probable ground state of the system. So the presentation here incorporates randomness as a key ingredient of the model.

It may be easily checked that the eigenvector corresponding to  $\lambda_{\min}$  prescribes the distribution of  $L$  and  $S$  tiles of a Fibonacci chain (up to our chosen sign convention). This corroborates the observations made in Section 3.3 earlier that the attractor of the chain is the Fibonacci state. In order to obtain the Fibonacci chain

**Table 1.**  $\text{rank}(\mathcal{H})$  vs  $N$ .

Length of chain, $N$	$\text{rank}(\mathcal{H})$
5	2
8	4
13	8
21	12
34	21
55	33
89	55
144	88
233	144

exactly in terms of the signed unitary digits,  $-1$  and  $1$  (and not only in their relative distribution of signs), a superposition of the relevant eigenvectors of  $\mathcal{H}$  must be considered. Thus, if one were to posit the Fibonacci state as a quantum state, the Fibonacci state  $\psi_F$  may be written as a linear superposition of  $r+1$  eigenvectors corresponding to the  $r+1$  dominant eigenvalues (including the zero eigenvalue) of the matrix  $\mathcal{H}$  whose rank is  $r < N$ , resulting in the following ansatz,

$$\psi_F = \sum_{n \leq r+1} c_n \psi_n, \quad (15)$$

where the  $\psi_n$ s are the orthonormal eigenvectors of  $\mathcal{H}$  and  $\psi_F := \pm \frac{1}{\sqrt{N}} \text{sign } \psi_1$  (see Eqs. (17) and (18)). The Fibonacci state  $\psi_F$  is degenerate as manifested by the appearance of  $\pm$  in the ansatz because the choice of the labels  $L \rightarrow -1$  and  $S \rightarrow +1$  is arbitrary. Both  $\psi_F$  and  $-\psi_F$  are solutions of  $\mathcal{H}|\psi\rangle = E|\psi\rangle$  [54]. This underscores the fact that it is the relative ordering of the signs of the entries of  $\psi_1$  that essentially dictates the attractor configuration. Further, the matrix  $\mathcal{H}$  is rank deficient because the resulting truncated Fibonacci chain is not an exact quasicrystal but an *approximant* with periodicity equal to  $N$ . Only in the infinite length chain, a full rank matrix Hamiltonian can be obtained. Another interesting observation from Table 1 is that the  $\text{rank}(\mathcal{H})$  for a chain of length  $N$  (corresponding to, say, Fibonacci word  $S_m$ ) is equal to the length of the previous Fibonacci word ( $S_{m-1}$ ) except in some cases where the result is off by one due to numerical imprecision in computing the diagonalization of  $\mathcal{H}$  owing to infinitesimally small numbers involved resulting in roundoff errors. This is likely due to the manner in which the higher Fibonacci words may be generated recursively like  $S_m = S_{m-1}S_{m-2}$ ,  $\forall m \geq 2$  as mentioned earlier in equation (2).

It may be insightful to provide an analogy with quantum mechanical systems. The energy of the Fibonacci state can be obtained as

$$\langle \psi_F | \mathcal{H} | \psi_F \rangle = E_{\psi_F} = \sum_n |c_n|^2 E_n, \quad (16)$$

where  $E_n$  is the  $n$ th eigenvalue of  $\mathcal{H}$  and denotes the  $n$ th energy eigenstate and the coefficient  $|c_n|^2$  is the probability of being in state  $\psi_n$ . The latter demands the restriction  $\sum_{n \geq 1} |c_n|^2 = 1$ . It may be interesting to note that if

$|c_n|^2 = \frac{1}{N}$ , then the value of  $E_{\psi_F}$  would be the ensemble average of the energy eigenvalues prescribed by  $H_\Omega$  whence all the energy eigenstates are equally probable, i.e.  $NE_{\psi_F} = \sum_n E_n = \text{Tr}(\mathcal{H}) = H_\Omega$ . This equipartition of energy eigenmodes is a signature of the principle of eigenstate thermalization [55–57]. Further, while the energy eigenstates may be equally probable in occurrence, their magnitudes are distinctly different because  $|E_1| > |E_2| > |E_3| >$  and so on, unless there is a degeneracy of eigenstates. In the present case, as is shown below,  $|E_1| \gg |E_i| \quad \forall i \neq 1$  which guarantees the prominence of the most relevant eigenstate  $\psi_1$ . In the next section, we will discuss if the condition of equiprobable eigenstates, given above, holds or not in the large  $N$  *thermodynamic* limit; and if not, what inference one may draw. In summary, two questions remain central to the inquiry in this paper.

- How to find the attractor of the Hamiltonian model?
- Why does the attractor configuration coincide with the Fibonacci chain as demonstrated by the simulations of the previous section?

The answer to the first question is essential to justify the observations of the simulations presented in Section 3.3. The answer to the second question is important in order to understand the physics of quasicrystal growth and the origin of aperiodicity in physical systems.

#### 4.2.3 How to find the attractor of the Hamiltonian?

Simulations of Section 3 prescribe a solution strategy for finding the attractor configuration. Is this attractor solution consistent with our quantum mechanical interpretation of the system? The central idea to find the explicit form of the solution of the final relaxed state of the Hamiltonian (12) is postulated as a superposition of eigenstates (15). Recall the ansatz (15): the attractor configuration is prescribed by sign  $\psi_1$  where  $\psi_1$  is the eigenvector corresponding to the most dominant energy eigenvalue  $E_1$  and sign is the well known signum function. Since the eigenvector corresponding to the most dominant eigenvalue prescribes the distribution of the tiles in the final state up to the chosen sign convention, the exact form of the final Fibonacci state of the chain can be obtained by writing a linear combination of the first  $(r+1)$  eigenvectors with the associated coefficients as mentioned in the expression (15). This will prescribe the correct exact form of the attractor configuration provided

$$\langle \mathbf{c}_{r+1}, \mathbf{c}_{r+1} \rangle = \sum_{i=1}^{r+1} |c_i|^2 = 1,$$

where  $\mathbf{c}_{r+1} = (c_1, c_2, c_3, \dots, c_r, c_{r+1})^T$ . Importantly, this attractor turns out to be the Fibonacci chain of length  $N$ . Figure 5 presents the values of  $\sum_{i=1}^{r+1} |c_i|^2$  for chains of different lengths by considering only the first  $(r+1)$  coefficients. In all cases, the value of  $\sum_{i=1}^{r+1} |c_i|^2$  is very close to

unity thereby validating the suitability of equation (15) to find the exact solution of the final relaxed state of the Hamiltonian. The solution obtained is the Fibonacci chain.

The solution strategy mentioned above is explained here through an example. Consider a chain of length  $N = 13$ . Under similarity transformation,  $\mathcal{H} = \Psi D \Psi^{-1}$  and the rank of  $\mathcal{H}$  is  $r = 8$ . The attractor of this system is obtained by considering the eigenvector

$$\psi_1 = \begin{pmatrix} 0.1962 \\ -0.1962 \\ 0.2917 \\ 0.2403 \\ -0.1941 \\ 0.5313 \\ -0.1455 \\ 0.1455 \\ 0.3860 \\ -0.2452 \\ 0.4366 \\ 0.0954 \\ -0.0954 \end{pmatrix} \quad (17)$$

and using the following ansatz and solving for the coefficients  $c_n$ ,

$$\frac{-1}{\sqrt{13}} \text{sign } \psi_1 = \frac{-1}{\sqrt{13}} \begin{pmatrix} 1 \\ -1 \\ 1 \\ 1 \\ -1 \\ 1 \\ -1 \\ 1 \\ 1 \\ -1 \\ 1 \\ 1 \\ -1 \end{pmatrix} = \sum_{n \leq 8+1} c_n \psi_n. \quad (18)$$

This gives us

$$\mathbf{c}_{r+1} = \begin{pmatrix} c_1 \\ c_2 \\ c_3 \\ c_4 \\ c_5 \\ c_6 \\ c_7 \\ c_8 \\ c_9 \end{pmatrix} = \begin{pmatrix} -0.8873 \\ -0.0335 \\ 0.0107 \\ -0.1524 \\ -0.2994 \\ 0.2110 \\ 0.1909 \\ -0.1328 \\ 0.0000 \end{pmatrix}$$

whence it may be checked that indeed

$$\langle \mathbf{c}_{r+1}, \mathbf{c}_{r+1} \rangle = \sum_{i \leq 8+1} |c_i|^2 = 1.$$

Finally, the attractor configuration  $\psi_F$  is expressed as a superposition of eigenstates (15) by using the coefficients computed above. This solution corresponds to the sixth

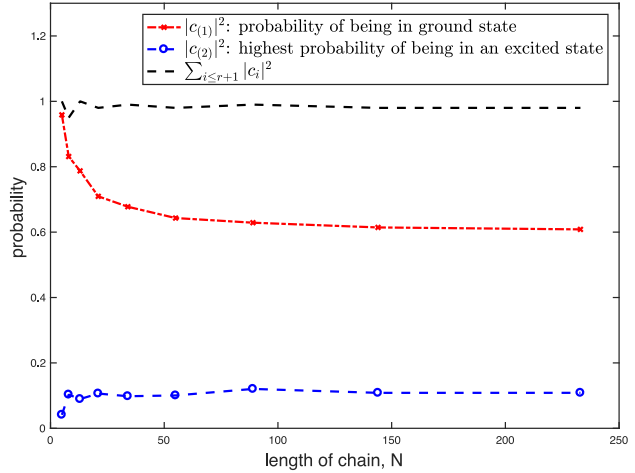


**Fig. 5.** This plot shows that the probability of the Fibonacci state being the ground state is significantly higher than being in any other excited state. It may be interesting to point out that the probability of being in the ground state asymptotically approaches the value of the golden ratio  $\phi$ . Further, it is shown that the solution prescribed by equation (15) is consistent with the fundamental axiom of probability,  $\sum_{i \leq r+1} |c_i|^2 = 1$ .

Fibonacci word  $S_5$  which can be found using the algorithmic recursion  $S_n = S_{n-1}S_{n-2}$ ,  $n \geq 2$ ,  $S_0 = 0, S_1 = 01$ . This paper presents a *physical* model of the emergence of Fibonacci quasicrystal that can also be constructed algorithmically as explained in several papers cited earlier. The solution of  $\mathcal{H}$  is an NP-hard optimization problem that essentially involves finding the most probable ground state energy [54,58,59].

#### 4.2.4 Why is the attractor configuration given by the Fibonacci chain?

While the ansatz allows us to find the attractor solution consistent with the postulates of quantum mechanics, a natural question that follows is: *why is the attractor configuration given by the Fibonacci chain?* After all, shouldn't one expect the relaxation of the Hamiltonian reminisce thermalization resulting in equipartition of energy among the different eigenstates? In fact, to the contrary, eigenstate thermalization would imply the absence of an attractor solution as multiple final states would be equally probable. So if one is looking for an attractor as a solution, and consequently a model of quasicrystal growth, thermalization is undesirable. So it works to our advantage that the Hamiltonian  $\mathcal{H}$  does not thermalize to equiprobable eigenstates.

In fact, let us rewrite the spectral decomposition given by equation (16) as

$$E_{\psi_F} = \sum_n |c_n|^2 E_n = \sum_{(m)} |c_{(m)}|^2 E_{(m)}, \quad (19)$$

where by convention  $|c_{(1)}|^2 \geq |c_{(2)}|^2 \geq |c_{(3)}|^2 \geq \dots$  and  $E_{(m)} \in \rho(\mathcal{H})$  (spectrum of  $\mathcal{H}$ ) is such that its coefficient is  $c_{(m)}$ . In other words, the second equality is

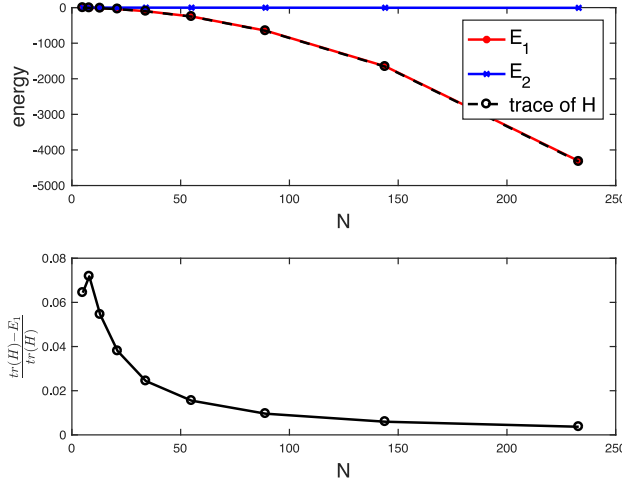


**Fig. 6.** Top: energy eigen values  $E_1$  and  $E_2$  of the Hamiltonian  $\mathcal{H}$  are plotted along with the trace of the Hamiltonian which gives the total energy of the system. Clearly,  $|E_1| \gg |E_2|$ . Bottom: this plot shows that the relative error in the approximation of  $Tr(\mathcal{H})$  by  $E_1$  decreases as  $N$  increases and is practically minuscule. The plots show that for moderately large  $N$ ,  $Tr(\mathcal{H})$  can be well approximated by  $E_1$ .

simply a re-arrangement of the summands in  $\sum_n |c_n|^2 E_n$  that obeys the above inequalities and sorts the energy eigenstates in decreasing order of the probability of finding the Fibonacci chain in that state. It turns out that  $c_{(1)} \equiv c_1$  and consequently  $E_{(1)} \equiv E_1$ . More importantly, the Hamiltonian  $\mathcal{H}$  is such that  $|c_{(1)}|^2 \gg |c_{(2)}|^2$  as shown clearly in Figure 5. In Section 3, we have presented results of numerical experiments that established that of all the possible configurations, it is the Fibonacci configuration that minimizes the total Hamiltonian  $H_\Omega = Tr(\mathcal{H})$ . Note that practically almost all of the total energy of the system is concentrated in the ground state as illustrated by Figure 6. In essence, since  $E_1 \rightarrow H_\Omega$  as  $N$  becomes large enough, it follows that the Fibonacci configuration not only minimizes  $H_\Omega$  among all possible chain configurations but also minimizes the ground state energy among all possible chain configurations. This establishes that the Fibonacci chain is the *most probable* ground state of the Hamiltonian  $\mathcal{H}$  and by a big margin (see Fig. 5).

It must be emphasized here that the ability of the empires, through simple non-local interactions as prescribed by the r.h.s. of equations (12) and (14), to form the final Fibonacci state of the chain renders the empires as the generators of the Fibonacci chain and fundamental elements in a model of aperiodic order. It can be shown that the simple nearest neighbor Ising model does not generate the Fibonacci chain.<sup>6</sup> Essentially, it is the *non-local* scope of the empires that is the quintessential element of the model.

### 4.3 Symmetries and comparison with the Ising model

The most fundamental symmetry in crystalline structures is translation symmetry. This symmetry is absent in quasicrystalline structures. In the current case under investigation here, the precise algebraic form in which a translation asymmetry pertaining to the Fibonacci quasicrystal may be conceptualized is illustrated by equations (9), (10) and (11). These empires collectively characterize all forbidden configurations of the Fibonacci chain. The Hamiltonian  $\mathcal{H}$  encodes the exact physical mechanism which manifests this translation asymmetry through the interaction of the empires.

Of course, this beckons a natural comparison with other lattice models especially with the most widely-known nearest neighbor Ising Hamiltonian. At the outset, it must be clarified that the Monte Carlo simulation of the nearest neighbor Ising Hamiltonian, that relies entirely on local spin–spin interactions, does not generate the Fibonacci chain or any one dimensional quasicrystal. This clearly underscores the necessary role of non-local interactions in a model of quasicrystal growth.

The definition of the empires (as illustrated by the examples (5) and (6), and the top and bottom figures on the left panel of Fig. 3) imply that the inner product  $J_{m,n} \langle \mathbf{E}_{\alpha_m} | \mathbf{E}_{\alpha_n} \rangle$  in equation (12) is essentially equivalent to  $\sum_{i=1}^N J_{m,n}^i s_i^m s_i^n = \sum_{i=1}^N J_{m,n}^i s_i^2$  because  $s_i^m = s_i^n = s_i$  where  $s_i$  labels the  $i$ th tile of the chain under consideration. Hence, one may attempt to devise an equivalent zero-field lattice model of the form

$$\begin{aligned} H_\Omega^{(1)} &= -\frac{1}{N} \sum_{m,n \in X} \sum_{i=1}^N J_{m,n}^i s_i^m s_i^n \\ &= -\frac{1}{N} \sum_{m,n \in X} \sum_{i=1}^N J_{m,n}^i s_i s_i \\ &= -\frac{1}{N} \sum_{m,n \in X} \sum_{i=1}^N J_{m,n}^i s_i^2 \end{aligned} \quad (20)$$

that generates the Fibonacci chain. Here  $s_i = \pm 1$  and  $J_{m,n} \equiv J_{m,n}^i$  is a vector for every  $m$  and  $n$  with non-zero unit entries at locations where the effect of the spins ( $s_i^2$ ) must be accounted for. Note that in the above equation we are no longer using the Einstein's summation convention. A careful observation of the interaction terms in the Hamiltonian (12) and the definition of the empire vectors reveals the formal similarities with the Hamiltonian (20). However, such an attempt to engineer the coupling constants does not encode the information of the projection from a higher dimensional space. Moreover, there does not appear a simple way to construct the coupling constants  $J_{m,n}^i$  and hence using model (20) to perform the analysis and the simulations, instead of the equivalent models (12) and (14), would be very challenging. On the other hand, the empires provide us with a tool to model non-local interactions very naturally and share a geometrical significance as the generators of the Fibonacci chain because they are derived by projection from a higher

<sup>6</sup> [https://www.youtube.com/watch?v=N85\\_aDD\\_lUI](https://www.youtube.com/watch?v=N85_aDD_lUI)

dimension which has translation symmetry. In any case the model (12) presented here is clearly *not* an Ising model for reasons mentioned above.

Like the nearest neighbor Ising model, the Hamiltonian  $H_\Omega$  is invariant under spin inversion as mentioned earlier. This is so because the inner product between the empire vectors is invariant under spin inversion. Eg., consider  $\mathbf{E}_{\alpha_m} = (s_1 s_2 s_3 \cdots s_N)$  and  $\mathbf{E}_{\beta_n} = (s'_1 s'_2 s'_3 \cdots s'_N)$  where  $s_i, s'_i = -1, 1$  or 0 depending on  $x_i = L, S$  or if it is an unforced tile. Clearly, the spin inversion  $s_i \rightarrow -s_i$  and  $s'_i \rightarrow -s'_i$ , which is essentially flipping the labels of  $L$  and  $S$ , preserves  $\langle \mathbf{E}_{\alpha_m} | \mathbf{E}_{\beta_n} \rangle$ .

However, unlike the zero external field nearest neighbor Ising model in one-dimension or the nearest neighbor Ising model in a square lattice in two-dimensions, the zero-external field ( $B_{\alpha_k, i} = 0$ ) partition function  $Z_\Omega = \text{Tr}(e^{-\beta H_\Omega})$  based on equation (12), and thereby the free energy density, are not invariant under sign inversion of the coupling coefficients  $J_{j,i}$ . This is because the non-zero entries of the interacting empire vectors change sign concurrently. This is further illustrated by the equivalent model (20). Therefore, the thermodynamic properties of the model presented here are not the same under the reversal of sign of the coupling constants  $J_{j,i}$ .

## 5 Summary of main results

The main contributions are summarized below.

- Algebraic forms of the empires of the VCs of a Fibonacci chain are provided. The closed form expressions are verified in agreement with earlier known methods of computing empires of VCs using geometric and algorithmic methods. These algebraic forms enable us to know the exact manner by which the translation symmetry is absent in a Fibonacci chain.
- A Hamiltonian is constructed using the empires mentioned above and Monte Carlo simulations are performed. The simulations show that the Fibonacci chain is an attractor of the model.
- The Hamiltonian is promoted to a matrix operator form and a spectral analysis is performed to find the relevant eigenstates. An ansatz is provided to find the attractor configuration analytically. It is verified to be true and consistent for a chain of any finite length. A quantum mechanical interpretation reveals that the Fibonacci chain is the most probable ground state of the system and hence provides a theoretical explanation of the attractor configuration. The theoretical analysis shows that the Fibonacci configuration not only minimizes the total energy of the system but also minimizes the ground state of the system.

We have devised a matrix Hamiltonian model of the Fibonacci quasicrystal. This approach may lay the foundation for formulating similar matrix models of more complex higher dimensional quasicrystals.

## 6 Future work

Firstly, there seems a formative correspondence between the empire Hamiltonian presented in this paper and the well known spin-1 Ising model with the spin-1 angular momentum matrices  $L^x, L^y, L^z$ , each of dimension  $3 \times 3$ , and with diagonal entries of  $L^z$  as 1, 0, -1. [60, 61]. This similarity stems from the use of ternary elements {1, -1, 0}. One may propose the following zero-field Hamiltonian

$$\mathcal{H}^{(*)} = - \sum_{a=\{x,y,z\}} \sum_{m,n \in X} J_{m,n} \mathcal{L}_m^a \mathcal{L}_n^a \quad (21)$$

as a *non-local* generalization of the spin-1 nearest neighbor Hamiltonian. Here,  $a, b = 1, 2, 3$  correspond to  $x, y, z$  and  $J_{m,n}$  are the non-local coupling constants between lattice sites  $m$  and  $n$ . By defining  $\mathcal{L}_m^a := I^{\otimes m-1} \otimes L^a \otimes I^{\otimes N-m}$ ,  $a = x, y, z$ , as  $3^N \times 3^N$  matrices and appropriately engineering  $J_{m,n}$ , one may investigate the correspondence between  $\mathcal{H}^{(*)}$  and  $\mathcal{H}$  given by equation (14). Here  $I$  is a  $3 \times 3$  identity matrix.

Secondly, the one-dimensional model described here may be extended to a two dimensional model of quasicrystal by relaxing a *network* of chains (fibers). The network of chains may be relaxed using a Monte Carlo simulation under specific topological constraints to obtain a matrix model of a two dimensional quasicrystal. A Fibonacci topological network based on a quantum string-net Hamiltonian has been studied recently [62].

The first author wishes to acknowledge some useful discussions with Raymond Aschheim regarding empires of vertex configurations. The second author wishes to thank Meredith Bowers for her support. Prashant Singh Rana and Rajendra Kumar Sharma of Thapar Institute are acknowledged gratefully for providing us access to their advanced computing laboratories that enabled us to perform some of the simulations and analysis presented in the revised version of the manuscript. The authors would also like to acknowledge the generous hospitality of Narendra Sharma and his team of Thapar Institute for making the stay of the second author a very pleasant experience. Finally, the authors would like to thank one anonymous referee for comments and suggestions to improve this paper.

## Author contribution statement

Both authors were involved in the development of the model and in the preparation of the manuscript. Both authors have read and approved the final manuscript.

**Publisher's Note** The EPJ Publishers remain neutral with regard to jurisdictional claims in published maps and institutional affiliations.

## References

1. M. Senechal, *Quasicrystals and Geometry* (Cambridge University Press, 1995)

2. M. Baake, U. Grimm, *Aperiodic Order: Volume 1, A Mathematical Invitation* (Cambridge University Press, 2013)
3. C. Janot, *Quasicrystals - A Primer* (Oxford University Press, 1994)
4. S. Ostlund, P.J. Steinhardt, *The Physics of Quasicrystals* (World Scientific Publishing Co., 1987)
5. D.J. Gross, Proc. Natl. Acad. Sci. USA **93**, 14256 (1996)
6. K. Brading, E. Castellani, *Symmetries in Physics: Philosophical Reflections* (Cambridge University Press, 2003)
7. H. Genz, Interdiscipl. Sci. Rev. **24**, 129 (1999)
8. R. Lifshitz, Isr. J. Chem. **51**, 1156 (2011)
9. A. Katz, M. Duneau, Scr. Metall. **20**, 1211 (1986)
10. H.C. Jeong, P.J. Steinhardt, Phys. Rev. B **55**, 3520 (1997)
11. H.C. Jeong, Phys. Rev. Lett. **98**, 135501 (2007)
12. U. Gaenshirt, M. Willsch, Philos. Mag. **87**, 3055 (2007)
13. A. Haji-Akbari, Nat. Lett. **462**, 773 (2009)
14. W. Steurer, Z. Anorg. Allg. Chem. **637**, 1943 (2011)
15. A. Kiselev, M. Engel, H.R. Trebin, Phys. Rev. Lett. **109**, 225502 (2012)
16. P. Vignolo, M. Bellec, J. Bohm, A. Camara, J.M. Gambaudo, U. Kuhl, F. Mortessagne, Phys. Rev. B **93**, 075141 (2016)
17. A. Sen, R. Aschheim, K. Irwin, Mathematics **5** (2017)
18. J. Bohsung, H.R. Trebin, Defects in Quasicrystals, in *APERIODICITY AND ORDER 2: Introduction to the Mathematics of Quasicrystals* (Academic Press Inc., 1989)
19. M. Oxborrow, C.L. Henley, Phys. Rev. B **48**, 6966 (1993)
20. I. Blinov, Sci. Rep. **5**, 11492 (2015)
21. M. Dzugutov, Phys. Rev. Lett. **70**, 2924 (1993)
22. M. Engel, P.F. Damasceno, C.L. Phillips, S.C. Glotzer, Nat. Mater. **14**, 109 (2015)
23. M. Engel, Dynamics and Defects of Complex Crystals and Quasicrystals: Perspectives from Simple Model Systems, PhD thesis, 2008
24. A.S. Keys, S. Glotzer, Phys. Rev. Lett. **99**, 235503 (2007)
25. K. Nagao, T. Inuzuka, K. Nishimoto, K. Edagawa, Phys. Rev. Lett. **115**, 075501 (2015)
26. M. Schmiedeberg et al., Phys. Rev. E **96**, 012602 (2017)
27. G. Onoda, P.J. Steinhardt, D.P. DiVincenzo, J.E.S. Socolar, Phys. Rev. Lett. **60**, 2653 (1988)
28. J.E.S. Socolar, Growth Rules for Quasicrystals, in *Quasicrystals - The State of the Art*, edited by D.P. DiVincenzo, P.J. Steinhardt (World Scientific, 1999)
29. R. Penrose, Tilings and Quasi-Crystals; a Non-Local Growth Problem, in *APERIODICITY AND ORDER 2: Introduction to the Mathematics of Quasicrystals* (Academic Press Inc., 1989)
30. S. Dworkin, J.I. Shieh, Commun. Math. Phys. **168**, 337 (1995)
31. G. van Ophuysen, Non-Locality and Aperiodicity of d-Dimensional Tilings, in *Quasicrystals and Discrete Geometry*, edited by J. Patera (American Mathematical Society, 1998)
32. R. Merlin, K. Bajema, R. Clarke, Phys. Rev. Lett. **55**, 1768 (1985)
33. M.W.C. Dharma-wardana, A.H. MacDonald, D.J. Lockwood, J.M. Baribeau, D.C. Houghton, Phys. Rev. Lett. **58**, 1761 (1987)
34. A. Dareau, E. Levy, M.B. Aguilera, R. Bouganne, E. Akkermans, F. Gerbier, J. Beugnon, Phys. Rev. Lett. **119**, 1 (2017)
35. J. Bellissard, B. Iochum, E. Scoppola, D. Testard, Commun. Math. Phys. **125**, 527 (1989)
36. A. Ghosh, S. Karmakar, Eur. Phys. J. B **11**, 575 (1999)
37. D. Tanese, E. Gurevich, F. Baboux, T. Jacqmin, A. Lemaitre, E. Galopin, I. Sagnes, A. Amo, J. Bloch, E. Akkermans, Phys. Rev. Lett. **112**, 146404 (2014)
38. N. Macé, A. Jagannathan, F. Piéchon, Phys. Rev. B **93**, 205153 (2016)
39. A. Mukherjee, A. Nandy, A. Chakrabarti, Eur. Phys. J. B **90**, 52 (2017)
40. W. Chuan, Fibonacci Q. **33** (1995)
41. W. Chuan, Subwords of the Golden Sequence and the Fibonacci Words (Springer, Dordrecht, 1996)
42. N.G. de Bruijn, Indagationes Math. **43**, 39 (1981)
43. B. Grunbaum, G. Shephard, *Tilings and Patterns* (Dover Books on Mathematics, 1987)
44. A. Carbone, M. Gromov, P. Prusinkiewicz, *Pattern Formation in Biology, Vision and Dynamics* (World Scientific Publishing, 2000)
45. M. Gardner, *Penrose Tiles to Trapdoor Ciphers: And the Return of Dr Matrix (Spectrum)* (W.H. Freeman, NY, 1989)
46. L. Minnick, Honors thesis, Williams College, 1998
47. J.B. Healy, Honors thesis, Williams College, 2000
48. L. Effinger-Dean, Honors thesis, Williams College, 2006
49. D. Hammock, F. Fang, K. Irwin, Crystals **8**, 370 (2018)
50. F. Fang, D. Hammock, K. Irwin, Crystals **2017**, 225911 (2017)
51. N. Goldenfeld, *Lectures on phase transitions and the renormalization group* (Levant Books, 2005)
52. R.J. Baxter, *Exactly Solved Models in Statistical Mechanics* (Academic Press, London, 1982)
53. P. Fendley, book in preparation (2019), <http://users.ox.ac.uk/~phys1116/>
54. A. Lucas, Front. Phys. **2**, 1 (2014)
55. M. Srednicki, Phys. Rev. E **50**, 888 (1994)
56. M. Rigol, V. Dunjko, M. Olshanii, Nature **452**, 854 (2009)
57. M. Rigol, M. Srednicki, Phys. Rev. Lett. **108**, 110601 (2012)
58. Z. Bian, F. Chudak, R. Israel, B. Lackey, W.G. Macready, A. Roy, Front. Phys. **2**, 1 (2014)
59. N.D.L. Espriella, G.M. Buendia, J.C. Madera, J. Phys. Commun. **2**, 025006 (2018)
60. J. Oitmaa, A.M.A. von Brasch, Phys. Rev. E **67**, 172402 (2003)
61. T. Kaneyoshi, J. Phys. Soc. Jpn. **56**, 933 (1987)
62. P. Fendley, S.V. Isakov, M. Troyer, Phys. Rev. Lett. **110**, 260408 (2013)